Synthesis and Characterization of Na Doped ZnO Rods Grown by Simple Chemical Method

Sibel MORKOÇ KARADENİZ [1]*, Hatice Kübra BÖLÜKBAŞI ÇIPLAK [2], Ali Ercan EKİNCİ [1]

[1] *Department of Physics, Faculty of Arts and Science, University of Erzincan Binali Yıldırım, Erzincan 24000, Turkey*
[2] *Graduate School of Natural and Applied Sciences, University of Erzincan Binali Yıldırım, Erzincan 24000, Turkey*

crossref http://dx.doi.org/10.5755/j01.ms.26.4.24227

Received 25 September 2019; accepted 25 November 2019

In this study, the effects of Na doped on the structure, morphology, and optical properties of the ZnO films deposited on glass substrate were investigated. The films were synthesized on glass substrates via a simple chemical method. Undoped and Na-doped ZnO films were obtained from an aqueous solution of the Zinc nitrate hexahydrate ($Zn(NO_3)_2 \cdot 6H_2O$), Sodium Nitrate ($NaNO_3$) and hexamethylenetetramine-HMT ($C_6H_{12}N_4$). Characterization of the films was examined using a Scanning electron microscope (SEM) and X-ray diffractometer (XRD), Ultraviolet-Visible spectrophotometer (UV-Vis) and X-Ray Photoelectron (XPS). The structure, morphology, and optical properties of the films were presented. The wurtzite ZnO films showed rod arrays morphology. The optical band gap increased with the doping of Na metal. The result shows that Na addition affected the properties of the ZnO films.
Keywords: ZnO, micro-nanorods, chemical deposition.

1. INTRODUCTION

Nanostructures such as rods [1], tetrapods [2] needles [3], tubes [4], belts [5] and wires [6] are among the most promising nanostructures because of their unique properties in various device applications.

1D nanostructured ZnO semiconductors with wide-bandgap are important components in optoelectronic and electronic devices such as solar cells [7, 8].

There are several methods to synthesize ZnO nanostructures, such as sol-gel [9], sputtering [10], ALD [11], chemical vapor deposition [12] and solvo-hydrothermal [13] methods. However, most of the techniques involve rigid conditions for instance high temperature, long reaction time [8].

The Chemical Bath Deposition (CBD), which is a simple and effective method for the synthesis of ZnO thin films, is based on the controlled chemical reaction in solution which leads to the formation of the films [14, 15].

One of the best ways to improve the physical properties of ZnO nanostructures is to doping [16].

Properties of the ZnO such as electrical conductivity, transmittance can be changed by the doping of ZnO and Alkali metals are better dopants than group-V elements because of shallowness of the acceptor level [16, 17].

In this study, the effect of Na addition on structural, optical and morphological properties of the ZnO films was investigated. The films are obtained by a simple, quick, one-step chemical method in a convection oven.

2. EXPERIMENTAL DETAILS

The chemical method was used for synthesizing undoped and Na doped ZnO films. In the CBD method, the deposition parameters such as pH of the bath, temperature of the bath, concentration of the bath, strongly affect morphological, optical, structural properties of the ZnO film and deposition process occurs [15-18]. The deposition reactions of undoped ZnO films synthesized with the method are given as follows:

$$Zn(NO_3)_2 \rightarrow Zn^{2+} + 2NO_3^-; \quad (1)$$

$$(CH_2)_6N_4 + 6H_2O \rightarrow 6HCHO + 4NH_3; \quad (2)$$

$$NH_3 + H_2O \rightarrow NH_4^+ + OH^-; \quad (3)$$

$$Zn^{2+} + 4NH_3 \rightarrow Zn[(NH_3)_4]^{2+}; \quad (4)$$

$$2H_2O \rightarrow H_3O^+ + OH^-; \quad (5)$$

$$Zn^{2+} + 2OH^- \rightarrow Zn(OH)_2; \quad (6)$$

$$Zn(OH)_2 \rightarrow ZnO + H_2O. \quad (7)$$

The films were synthesized on unseeded glass substrates. The glasses were cleaned with Acetone (15 min), 2-Propanol (15 min), deionized water (15 min) in an ultrasonic cleaner. The clean substrates were dried in an air oven at 70 – 80 °C. $Zn(NO_3)_2 \cdot 6H_2O$, $NaNO_3$, and $C_6H_{12}N_4$ (HMT) were used for preparing the bath solution. $NaNO_3$ was doped as a 10 % mole of $Zn(NO_3)_2 \cdot 6H_2O$ precursor. The substrates were dipped in the bath. The reaction was achieved at 100 °C in 4 hours in a convection oven. After the deposition process, the samples were annealed at 400 °C for 2 hours.

The properties of the ZnO arrays were analyzed by means of Panalytical Empyrean Model X-ray diffractometer, FEG Quanta 450 Scanning Electron Microscope, TETRA T80+ Uv/Vis Spectrophotometer and Specs-Flex model X-Ray Photoelectron Spectrometer.

*Corresponding author. Tel.: +90-446-2243032; fax: +90-446-2243016.
E-mail address: *morkocsibel@gmail.com* (S. Morkoç Karadeniz)

3. RESULTS AND DISCUSSION

The X-ray diffraction pattern, which gives information about the crystal structure of the material, exhibits some changes such as intensity, diffraction angle due to the doping of a different ion to the structure or due to the replacement of the present ion (Zn^{2+}) with a foreign ion having a different ionic radius. Any doping element replaces the present ion (Zn^{2+}) or selects crystal defect points. As a result, any X-ray diffraction peak intensity of the film belonging to orientation may increase or decrease. In addition, a slight shift in the XRD peak position (at the diffraction angle) may occur with doping ion in the structure. As is known from Bragg's law, the X-ray diffraction angle is directly proportional to the *d* lattice parameter. The intensity of each peak gives information about the structure of the lattice. It is possible to change the *d* and *a*, *c* lattice parameters directly proportional to the change in ionic radius with doping material in the structure. An increase in the ionic radius may result in an increase in the lattice parameters. The ionic radius is the radius of the ion in the ionic crystal structure. ZnO is a compound with II-VI group coordination and its ionic radius is 0.60 Å, however, this value is 0.99 Å for the Na^{+} ion to replace the Zn^{2+} ion [19]. The XRD patterns of the samples are shown in Fig. 1.

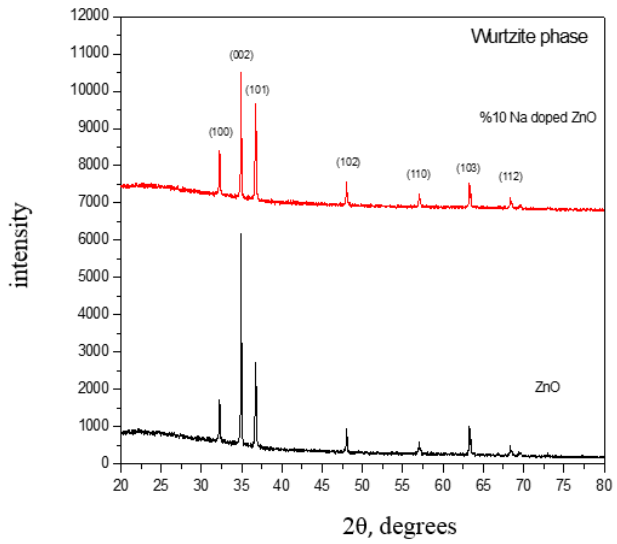

Fig. 1. XRD patterns of the ZnO films

Crystal structure of the films is in good agreement with the wurtzite ZnO crystal system (JCPDS No. 36-1451) [20]. The peak of ZnO films along (002) plane indicates maximum intensity. The maximum peak intensity of Na-doped ZnO film decreased compared to ZnO film and a small amount of shift occurred in the maximum peak position. Table 1 shows the *D* crystal grain size and the lattice parameters for the (002) plane. The particle size was calculated with the Scherer equation which is given as follows:

$$D = \frac{0.9\,\lambda}{\beta \cos\theta} \qquad (1)$$

where λ is the X-ray wavelength; *k* is the constant (0.9); θ is the Bragg angle and β is the full width at half maximum [14]. The grain size (*D*) decreased and the lattice parameters (*c*, *d*) increased slightly due to the increase in ionic radius with Na-addition. The lattice constants for the wurtzite ZnO were calculated by Eq. 2 [21]:

$$\frac{1}{d^2} = \left[\frac{4}{3} \times \frac{h^2+hk+k^2}{a^2}\right] + \frac{l^2}{c^2} \qquad (2)$$

Table 1. Lattice parameters and crystal grain size of the ZnO films

Sample	*a*, Å	*c*, Å	*d*-spacing, Å	*D*, nm
ZnO	3.2050	5.1380	2.5690	110
10 % Na doped ZnO	3.2048	5.1385	2.5692	96

SEM images of the ZnO are shown in Fig. 2.

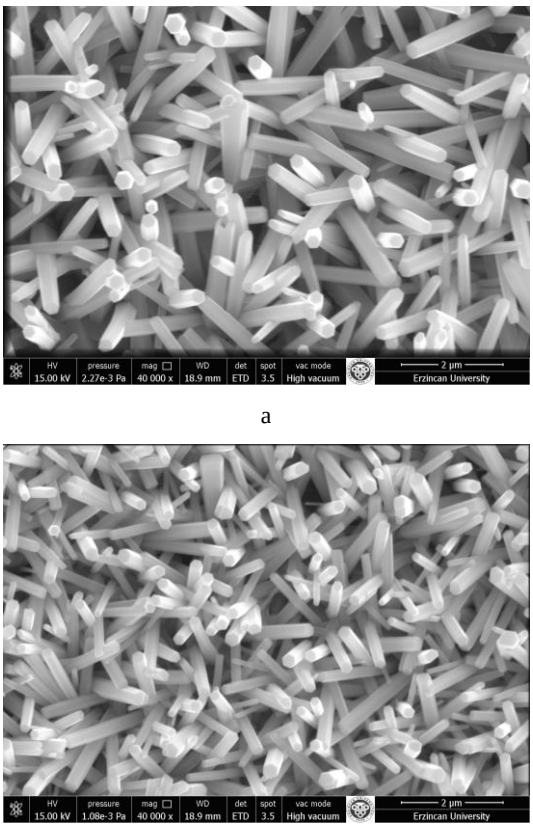

Fig. 2. SEM images of: a – un-doped; b – Na doped ZnO film

XPS spectra of the ZnO films are given in Fig. 3. The profile of peaks was taken as the Gaussian function. Binding energies of Zn $2p_{1/2}$, $2p_{3/2}$ O 1s were observed at 1019 eV, 1042 eV, 529.1 eV respectively. The 1019 eV, 1042 eV peaks of the Zn $2p_{1/2}$, $2p_{3/2}$ spectrum can be attributed to metallic Zn and 529.1 eV peak of the O1s spectrum can be attributed to the Zn–O bonds [24]. The photoemission peak located at around 1068.8 eV for Na 1s shows the doping of Na impurities in the atomic structure of ZnO. Therefore, the XPS results confirm that the Na element substituting for Zn [25]. The low binding energy component centered at 529.5 eV may be attributed to the oxygen atoms position of Na_2O.

UV/Vis absorption spectra of the ZnO films are shown in Fig. 4. Both of the films showed strong absorption in the UV region. However, Na-doped ZnO films showed enhancement of absorption spectra in the visible region.

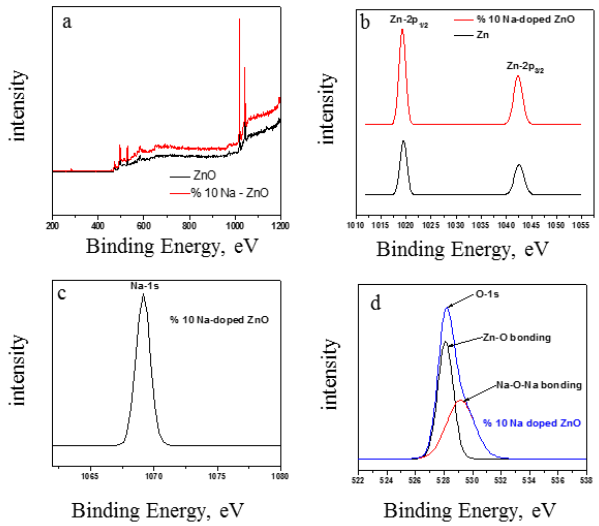

Fig. 3. a – survey XPS spectra of ZnO films; high-resolution XPS spectra of: b – Zn 2p; c – Na 1s, d – O 1s of the ZnO films

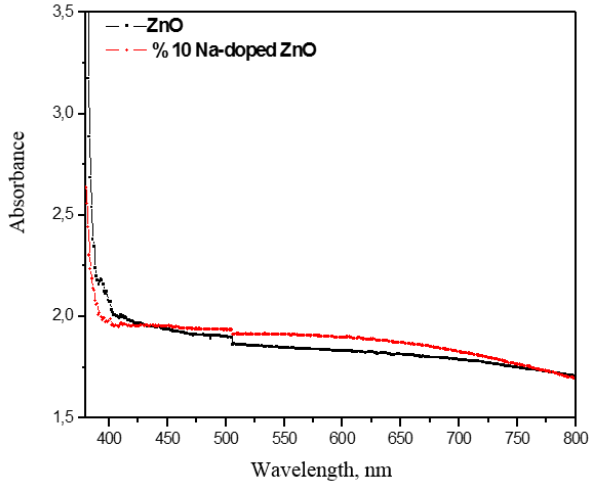

Fig. 4. UV-Vis absorption spectra of the ZnO films

The enhanced absorption is attributed to the interaction and the transfer of electrons between the Na and ZnO and the Surface Plasmon Resonance (SPR) absorption of Na ions [26]. Fig. 5 shows the energy bandgap of the ZnO films estimated by the extrapolation of the linear part of the $(ahv)^2$ versus hv plots. From the optical absorption spectra it was possible to determine the value of the energy gap (Eg) using Tauc Equation [27];

$$\alpha h\upsilon = A\left(h\upsilon - E_g\right)^n \quad (3)$$

Eq. 3 shows α absorption coefficient, E_g optical band gap, A constant and n = ½ for the allowed direct band, n = 2 or the allowed indirect band [28].

The energy band gap of ZnO film is obtained as ~ 3.25 eV. The Na-doped ZnO film showed an increase in the gap to around 3.34 eV. The increase in the bandgap is explained with the Moss-Burstein shift due to the increasing Fermi level in the conduction band [29].

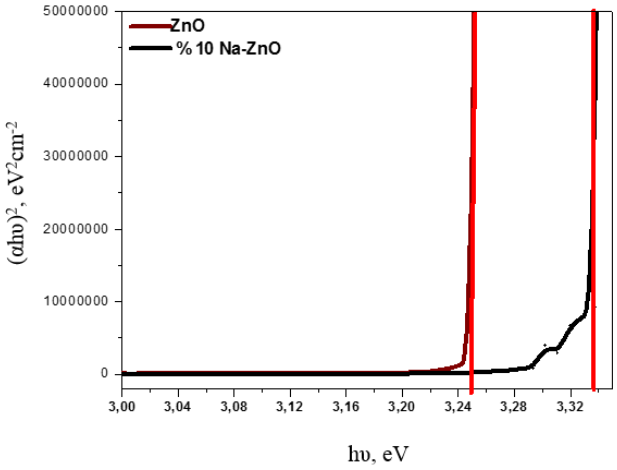

Fig. 5. The $(ahv)^2$ versus hυ curves for the optical band gap determination of the ZnO films

4. CONCLUSIONS

In this study, ZnO and Na-doped ZnO films were successfully prepared by a simple and fast one-step chemical method. XRD results showed that the ZnO films have a wurtzite phase with the maximum peak of (002) orientation.

The crystal grain size of the films was found as 110 and 96 nm respectively for undoped and Na-doped ZnO. Crystallite size decreased with Na addition. The average diameter of the rods decreased with Na doping. The absorbance increased with doping Na metal. The optical band gap values of the films were found around 3.25 and 3.34 eV respectively for undoped and Na-doped ZnO. Consequently, Na has successfully doped to the ZnO structure with a simple chemical method in a convection oven and its optical bandgap value widened with Na doping. So the Na doped ZnO rod arrays can exhibit higher performance than undoped ZnO rod arrays in many potential applications with widening bandgap.

Acknowledgments

Thanks to EUTAM and DAYTAM for XRD, SEM and XPS analyses.

REFERENCES

1. **Pourshaban, E., Abdizadeh, H., Golobostanfard, M.R.** ZnO Nanorods Array Synthesized by Chemical Bath Deposition: Effect of Seed Layer Sol Concentration *Procedia Materials Science* 11 2015: pp. 352 – 358. https://doi.org/10.1016/j.mspro.2015.11.124
2. **Rackauskas, S., Klimova, O., Jiang, H., Nikitenko, A., Chernenko, K.A., Shandakov, S.D., Kauppinen, E.I., Tolochko, O.V., Nasibulin, A.G.** A Novel Method for Continuous Synthesis of ZnO Tetrapods *Journal of Physical Chemistry C* 119 (28) 2015: pp. 16366 – 16373. https://doi.org/10.1021/acs.jpcc.5b03702
3. **Park, W.I., Yi, G.C., Kim, M., Pennycook, S.J.** ZnO Nanoneedles Grown Vertically on Si Substrates by Non-Catalytic Vapor-Phase Epitaxy *Advanced Materials* 14 (24) 2002: pp. 1841 – 1843. https://doi.org/10.1002/adma.200290015

4. **Xi, Y., Song, J., Xu, S., Yang, R., Gao, Z., Hu, C., Wang, Z.** Growth of ZnO Nanotube Arrays and Nanotube Based Piezoelectric Nanogenerators *Journal of Materials Chemistry* 19 (48) 2009: pp. 9260 – 9264. https://dx.doi.org/10.1039/b917525c
5. **Hai, N., Xiaodong, L.** Young's Modulus of Zno Nanobelts Measured Using Atomic Force Microscopy and Nanoindentation Techniques *Nanotechnology* 17 (14) 2006: pp. 3591 – 3597. https://dx.doi.org/10.1088/0957-4484/17/14/039
6. **Jingbiao, C.** Zinc Oxide Nanowires *Materials Characterizations* 64 2012: pp. 43 – 52. https://doi.org/10.1016/j.matchar.2011.11.017
7. **Ghoul, M., Braiek, Z., Brayek, A., Ben Assaker, I., Khalifa, N., Ben Naceur, J., Souissi, A., Lamouchi, A., Ammar, S., Chtourou, R.** Synthesis of Core/shell Zno/ZnSe Nanowires Using Novel Low Cost Two Steps Electrochemical Deposition Method *Journal of Alloys and Compounds* 647 2015: pp. 660 – 664. https://doi.org/10.1016/j.jallcom.2015.06.100
8. **Qi, L., Li, H., Dong, L.** Simple Synthesis of Flower-Like Zno by a Dextran Assisted Solution Route and their Photocatalytic Degradation Property *Materials Letters* 107 2013: pp. 354 – 356. https://doi.org/10.1016/j.matlet.2013.06.054
9. **Morandi, S., Fioravanti, A., Cerrato, G., Lettieri, S., Sacerdoti, M., Carotta, M.C.** Facile synthesis of ZnO Nano-structures: Morphology Influence on Electronic Properties *Sensors and Actuators B: Chemical* 249 2017: pp. 581 – 589. https://doi.org/10.1016/j.snb.2017.03.114
10. **Girija, K.G., Somasundaram, K., Topkar, A., Vatsa, R.K.** Highly Selective H_2S Gas Sensor Based on Cu-Doped Zno Nanocrystalline Flms Deposited by RF Magnetron Sputtering of Powder Target *Journal of Alloys and Compounds* 684 2016: pp. 15 – 20. https://doi.org/10.1016/j.jallcom.2016.05.125
11. **Zafar, M., Yun, J.Y., Kim, D.H.** Performance of Inverted Polymer Solar Cells with Randomly Oriented ZnO Nanorods Coupled with Atomic Layer Deposited ZnO *Applied Surface Science* 398 2017: pp. 9 – 14. https://doi.org/10.1016/j.apsusc.2016.11.211
12. **Barreca, D., Bekermann, D., Comini, E., Devi, A., Fischer, R.A., Gasparotto, A., Maccato, C., Sberveglieri, G., Tondello, E.** 1D ZnO Nano-Assemblies by Plasma-CVD as Chemical Sensors for flammable and Toxic Gases *Sensors and Actuators B: Chemical* 149 (1) 2010: pp. 1 – 7. https://doi.org/10.1016/j.snb.2010.06.048
13. **Moulahi, A., Sediri, F.** Controlled Synthesis of Nano-ZnO Via Hydro/Solvothermal Process and Study of their Optical Properties *Optik* 127 (19) 2016: pp. 7586 – 7593. https://doi.org/10.1016/j.ijleo.2016.05.128
14. **Morkoç Karadeniz, S, Bozkurt Çirak, B., Kilinç, T., Çirak, Ç., İnal, M., Turgut, Z., Ekinci, A.E., Ertuğrul, M.** A Comparative Study on Structural and Optical Properties of ZnO Micro-Nanorod Arrays Grown on Seed Layers Using Chemical Bath Deposition and Spin Coating Methods *Materials Science (Medžiagotyra)* 22 (4) 2016: pp. 476 – 480. http://dx.doi.org/10.5755/j01.ms.22.4.13443
15. **Shaik, S.K., Inamdar, S.I., Ganbavle, V.V., Rajpure, K.Y.** Chemical Bath Deposited ZnO Thin Film Based UV Photoconductive Detector *Journal of Alloys and Compounds* 664 2016: pp. 242 – 249**.** https://doi.org/10.1016/j.jallcom.2015.12.226
16. **Saáedi, A., Yousefi, R., Jamali-Sheini, F., Zak, A.K., Cheraghizade, M., Mahmoudian, M.R., Baghchesara, M.A., ShirmardiDezaki, A.** XPS Studies and Photocurrent Applications of Alkali-Metals-Doped ZnO Nanoparticles Under Visible Illumination Conditions *Physica E* 79 2016: pp. 113 – 118. https://doi.org/10.1016/j.physe.2015.12.002
17. **Mahdhi, H., Ayadi, Z.B., Gauffier, J.L., Djessas, K., Alaya, S.** Effect of Sputtering Power on the Electrical and Optical Properties of Ca-Doped ZnO Thin Films Sputtered From Nanopowders Compacted Target *Optical Materials* 45 2015: pp. 97 – 103. https://doi.org/10.1016/j.optmat.2015.03.015
18. **Tomoaki, T., Ashikyn, H.N., Azzyaty, J.N., Toshiya, W., Manaf, H.A., Masakazu, Y.** Shape Controlled Growth of ZnO Nanorods and Fabrication of ZnO/CuO Heterojunctions by Chemical Bath Deposition Using Zinc Nitrate Hexahydrate and Copper (III) Nitrate Trihydrate *Thin Solid Films* 596 2015: pp. 201 – 208. https://doi.org/10.1016/j.tsf.2015.07.082
19. **Akcan, D., Gungor, A., Arda, L.** Structural and Optical Properties of Na-Doped ZnO Films *Journal of Molecular Structure* 1161 201: pp. 299 – 305. https://doi.org/10.1016/j.molstruc.2018.02.058
20. **Tsai, J.K., Meen, T.H., Wu, T.C., Yu-Da Lai, Y.D., He, Y.K.** Morphology and Optical Properties of ZnO Microrods Grown by High-Temperature Hydrothermal Method *Microelectronic Engineering* 148 2015: pp. 55 – 58. https://doi.org/10.1016/j.mee.2015.08.006
21. **Mclaren, A., Valdes-Solis, T., Li, G., Tsang, S.C.** Shape and Size Effect of ZnO nanocrystals on Photocatalytic Activity *Journal of the American Chemical Society* 131 2009: pp. 12540 – 12541. https://doi.org/10.1021/ja9052703
22. **Morkoç Karadeniz, S., Özturan Yeşilyurt, M.** Chemically growth of ZnO rods arrays on non-seeded glass substrates *Surfaces and Interfaces* 18 2020: pp. 1– 4. https://doi.org/10.1016/j.surfin.2019.100418
23. **Kokotov, M., Hodes, G.** Reliable Chemical Bath Deposition of Zno Films with Controllable Morphology From Ethanolamine-Based Solutions Using $KMnO_4$ Substrate Activation *Journal of Materials Chemistry* 19 2009: pp. 3847 – 3854. https://dx.doi.org/10.1039/b821242b
24. **Tüzemen, E.Ş., Şahin, H., Kara, K., Elagöz, S., Debajeet, B., Esen, R.** XRD, XPS, and Optical Characterizations of Al-doped ZnO _lm Grown on GaAs Substrate *Turkish Journal of Physics* 38 2011: pp. 111 – 117. https://dx.doi.org/10.3906/fiz-1301-17
25. **Saáedi, A., Yousefi, R., Jamali-Sheini, F., KhorsandZak, A., Cheraghizade, M., Mahmoudian, M.R., Baghchesara, M.A., Dezaki, A.S.** XPS Studies and Photocurrent Applications of Alkali-Metals-Doped ZnO Nanoparticles Under Visible Illumination Conditions *Physica E* 79 2016: pp. 113 – 118. https://doi.org/10.1016/j.physe.2015.12.002
26. **Saoud, K., Al Soubaihi, R., Saeed, S., Bensalah, N., Al-Fandi, M., Singh, T.** Heterogeneous Ag and ZnO Based Photocatalytic For Waste Water Treatment Under Different Irradiation Conditions *Journal of Materials and Environmental Sciences* 9 2018: pp. 400 – 441. https://dx.doi.org/10.26872/jmes.2018.9.2.44

27. **Silva, E.P., Chaves, M., Durrant, S.F., Lisboa-Filho, P.N., Bortoleto, J.R.R.** Morphological and Electrical Evolution of ZnO:Al Thin Films Deposited by RF Magnetron Sputtering onto Glass Substrates *Materials Research* 17 2014: pp. 1384 – 1390. http://dx.doi.org/10.1590/1516-1439.281214

28. **Tatar, D., Güney, H.** Synthesis and Characterization of Zno:Ni Thin Films Grown by Spray Deposition *Ceramics International* 43 2017: pp. 16593 – 16599. https://doi.org/10.1016/j.ceramint.2017.09.047

29. **Aparna, T., Misha, H., Mathew, S., Ani, J.S., Erni, R., Debajeet, B., Artur, B., Nampoori, V.P.N.** Synthesis of Monocrystalline Zinc Oxide Microrods by Wet Chemical Method for Light Confinement Applications *Physica E* 44 (10) 2012: pp. 2118 – 2123. https://doi.org/10.1016/j.physe.2012.06.026